

Prediction of Time Variant Spatial Channel Impulse Responses for Wireless Ad-hoc Networks

René Wahl¹⁾, Gerd Wölfle¹⁾, Robert Weigel²⁾

¹⁾AWE Communications GmbH, Boeblingen, Germany, www.awe-communications.com

²⁾Friedrich-Alexander University Erlangen-Nuremberg, Germany, www.uni-erlangen.org

Abstract – With the growing demand for wireless communication systems, wireless concepts for the data exchange in time variant ad-hoc networks become more and more interesting. In order to describe and thus assess the mobile radio channels in such networks, simulations are required. The main aspect is the time-variance of the channel impulse response and the modeling of large scenarios. This paper discusses the demands for a model to describe the radio channel in time variant environments and presents an appropriate ray tracing approach. A new concept is introduced to substitute complex polygonal objects by several radar cross sections. The performance of the Ray Tracing algorithm is demonstrated by a comparison from predictions to measured channel characteristics.

Index Terms – Ad-hoc Networks, Ray Tracing, Time Variant, Radar Cross Section, Ray Optical, Vehicles, Cars, Car-to-Car Communication

I. INTRODUCTION

After the great success of wireless communications used in land mobile radio systems, wireless data exchange in time variant ad-hoc networks become interesting. The steadily increasing demand for mobile multimedia and safety applications requires looking for new concepts for the planning of wireless systems. Time variant scenarios can be found in several environments: Some examples are vehicular ad-hoc networks used for driving assistance systems or Wi-Fi hotspots in railroad stations, airports or city centers. The main aspect in such scenarios is the time variance of these environments, as the locations of either transmitter, receiver or of obstacles in these scenarios change continuously. These effects influence the propagation situation and lead to channel impulse responses, which are significantly affected by the time variance.

II. RAY OPTICAL PROPAGATION MODELING

A. Current Status

Ray optical propagation models are well known in the domain of urban radio network planning [1]. Ordinary urban scenarios are static; movements of objects and the consideration of time variant effects are not possible. However the vector databases can be modified manually for several snapshots to make them “dynamic”. But in this case time variant effects like the Doppler Shift are still not considered during prediction. This paper presents an approach which allows the consideration of time variance.

B. Time Variant Ad-hoc Networks

Some examples for time variant ad-hoc networks are given in the following:

- Connections between several mobile stations using the IEEE 802.11 protocol (WLAN ad-hoc mode).
- Vehicular Ad-hoc Networks (VANets, IEEE 802.11p) are used for the Car-2-Car Communication.
- Wi-Fi planning in airports or railroad stations, where many objects are time variant.

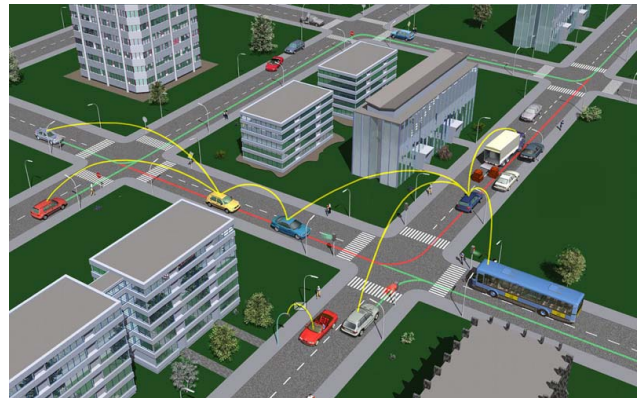


Fig. 1: An example for a wireless ad-hoc network: A Car-2-Car communication scenario [2].

This paper focuses mainly on vehicular ad-hoc networks (Car-2-Car), but the presented approach is also suitable for all other types of wireless ad-hoc networks. An example of a Car-2-Car communication scenario is depicted in Fig. 1. In real traffic situations, many objects influence the propagation of waves around vehicles. Buildings, vegetation, guardrails and other vehicles have a significant influence on the received channel impulse response (CIR).

C. Modelling of Scenarios and Vehicles

Each element in the scenario can be either stationary (not moving) or non-stationary (dynamic). In the approach presented in this paper, translation and rotation properties can be assigned to each object. For translation, a vector with the direction of the movement as well as a velocity must be defined. Rotation requires also a velocity, but additionally a rotation center. The behavior of the objects is defined by a list of different transformation properties, which are valid for certain distances. Both transformations together (translation and rotation) allow complex movements of objects.

Predictions with the Ray Tracing approach are then computed for arbitrary defined snapshot times. All time

variant objects in the scenario are moved to the correct time-dependent position for the current time stamp before the prediction starts. Two different approaches are supported for the modeling of objects in scenarios:

1) Polygons

The bases of a scenario are either planar polygons for complex objects or cylinders with polygonal ground plate for simple items. With this distinction it is possible to define all objects in a scenario from as simple as possible (buildings) to as highly accurate as needed (vehicles). Polygons can be defined with an arbitrary number of corners and they can be arbitrarily located in the scenario. Subdivisions are available, which allow the modeling of sub-elements like windows in metal frames (e.g. doors of cars). An individual material property (dielectricity, permeability and conductance) can be assigned to each polygon.

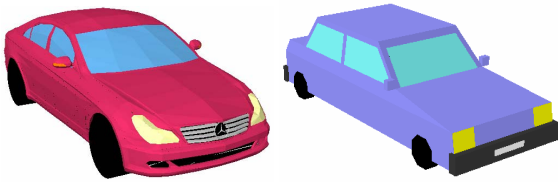


Fig. 2: Vector oriented databases of cars: Highly accurate model (left) and simple model.

Vector oriented 3D CAD data can be used to model cars. An example of both, a complex and a simple modeled car is shown in Fig. 2. As simple models consist of only some polygons, only a few diffractions and reflections occur on the car body. This is not consistent with the reality, because car bodies have bent surfaces, which lead to many reflections and diffractions. That is the reason why highly accurate models of cars have to be used for the predictions.

2) Radar Cross Sections

One problem using highly accurate 3D models of cars is the large memory amount, needed for each car model in the scenario. As these models consist of thousands of polygons, the computation time is also influenced in a negative way. Reflections and diffractions have to be computed on each polygon.

These restrictions lead to alternative ways of modeling vehicles. One way is to use radar cross sections (RCS) instead of polygonal descriptions. RCS defines a relation between each incident and each scattered ray/angle to an object. The relation used here is the full polarimetric description with a scattering matrix:

$$|S| = \begin{bmatrix} S_{vv}(\varphi_i, \theta_i, \varphi_s, \theta_s) & S_{vh}(\varphi_i, \theta_i, \varphi_s, \theta_s) \\ S_{hv}(\varphi_i, \theta_i, \varphi_s, \theta_s) & S_{hh}(\varphi_i, \theta_i, \varphi_s, \theta_s) \end{bmatrix}$$

The equation above shows the scattering matrix, defined for each combination of incident and scattered rays. Incident rays are characterized by the incident angles φ_i, θ_i and scattered rays are defined by φ_s, θ_s . In the special case of monostatic RCS data, the conditions $\varphi_i = \varphi_s$ and $\theta_i = \theta_s$ are fulfilled. For the scenarios focused in this paper, bistatic RCS are needed, as rays are often scattered in other directions as they have arrived from.

RCS data is available in four-dimensional arrays, because for each angle $\varphi_i, \theta_i, \varphi_s, \theta_s$ one dimension is needed. This leads to a large amount of memory, if a wide angular area for the incident and scattered angles is considered. Investigations have shown a lot of values of the data set are near to zero. This allows the usage of a sparse matrix algorithm [3], which leads to a justifiable amount of memory.

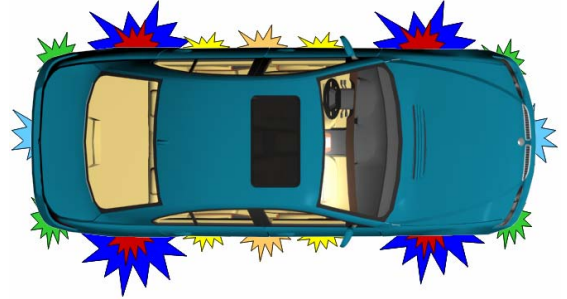


Fig. 3: A car substituted with 20 radar cross sections (RCS).

RCS are only valid in larger distances from transmitter and receiver, as the real object is reduced to one single scattering point in the RCS theory [5]. This is the reason, why a modeling with only one RCS per vehicle is not valid in typical dimensions of traffic scenarios. Thus, vehicles are substituted by not only one RCS, but by many RCS. In a first step, all relevant scattering centers of vehicles have to be extracted [6]. Afterwards the RCS have to be computed [7] or measured for these scattering centers. Investigations have shown a modeling with 20 RCS per vehicle leads to satisfying results (see Fig. 3). RCS are available for the four wheels (tires with rims), the four corners, the four fenders, the four doors and for the front, back and both side parts.

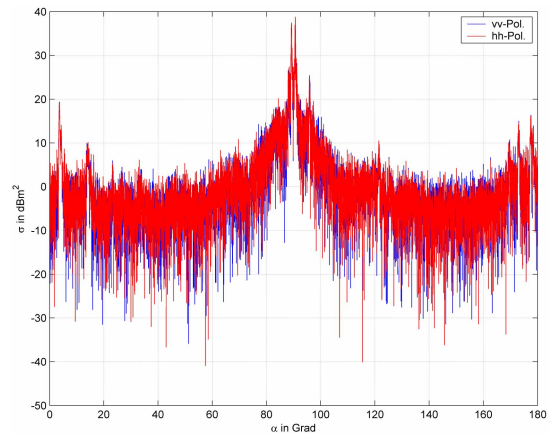


Fig. 4: Monostatic RCS in dBm² in a horizontal plane of a whole car. Computed by FGAN [4].

RCS data is not only available for cars, but also for pedestrians [7]. An example of a RCS of a whole car is shown in Fig. 4. The plot demonstrates the relation between incident and scattered angles $\varphi_i = \varphi_s$ for a fixed elevation angle $\theta_i = \theta_s = 90^\circ$.

D. Enhanced 3D Ray Tracing Algorithm

A new 3D Ray Tracing model has been developed for time variant scenarios. The algorithm supports an arbitrary number of reflections, scatterings and transmissions for

each ray path. Up to two diffractions are considered per ray path. Reflections are determined with the image theory and for the computation of the diffraction points an algorithm is implemented, which is based on permutation of all combinations of potential diffraction points. First, all potential diffraction wedges are divided into small sections and for each section a potential diffraction point in the center of the section is marked. During the computation with the Ray Tracing, the algorithm does always a loop over all potential diffraction points to check if a diffraction occurs for the current ray path or not. Diffraction only occurs if the angle criterion for incident and diffracted ray is fulfilled [9]. The attenuations caused by reflections and transmissions are determined with the Fresnel coefficients [10] and for the diffractions the Uniform Geometrical Theory of Diffraction (GTD/UTD) is used [11].

Scattering on rough surfaces is also included in the model. Therefore objects with rough surfaces are divided into small triangles. Each triangle delivers a scattering contribution to the CIR. The scattering point is placed in the center of the triangle. For the determination of the attenuation due to a scattering, measured or computed scattering matrixes, depending on incident and scattered azimuth angles, can be used. A measurement setup with a network analyzer was used to measure the scattering on different road surfaces and for different weather conditions. Fig. 5 shows an illustration of this setup. Tx is the radiating antenna and Rx is the receiver. Both angles, α and β , were varied from 0 to 60°. An absorber was used to suppress the Line-Of-Sight ray from Tx to Rx. The measured values are independent of the azimuth.

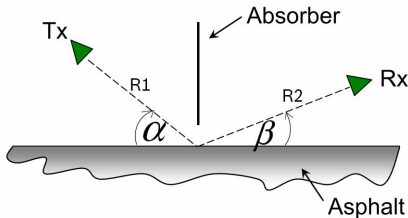


Fig. 5: Measurement setup with transmitter (Tx) and receiver (Rx) to measure the scattering behavior of asphalt.

The algorithm allows an unlimited number of interactions for each propagation path. All combinations of reflections, diffractions and scatterings (on RCS scattering centers and on road surfaces) are possible for each ray. Furthermore, RCS scattering centers and can interact with each other. This guarantees the consideration of interactions between different sections of vehicles.

E. Computed Results

The Ray Tracing algorithm computes the Channel Impulse Response (CIR) for each receiver location. Also available is the direction of arrival (DoA) for each receiver point, as well as the direction of departure (DoD) at the transmitter. A combination of CIR and DoA leads to the spatial channel impulse response.

The time variance of objects causes Doppler Shifts, if rays interact with moving objects. Especially for the design of receivers, it is evident to know the bandwidth of the signal at Rx. If a propagation path interacts with a time

variant object, e.g. a vehicle, the frequency of the propagating wave changes. The Doppler Shift is computed according to the following equation [12]:

$$f_D = \frac{v}{c} f \cos(\alpha)$$

The angle α is the angle between the direction of traveling of the time variant object and the arriving ray path. The relative velocity of the time variant object is denoted with v and c is the velocity of light. The frequency is denoted with f . The actual frequency changes every time a propagation path hits a time variant object. If the time variant object moves towards the propagating ray, the shift is positive, otherwise it is negative. The Ray Tracing algorithm considers the Doppler Shift for each ray, which interacts with moving objects. The Doppler Shift is also considered if the transmitter or the receiver is time variant.

The transmission matrix can be used for the characterization of the channel:

$$\begin{pmatrix} E_{\vartheta out} \\ E_{\varphi out} \end{pmatrix} = \begin{bmatrix} T_{11} & T_{21} \\ T_{12} & T_{22} \end{bmatrix} \begin{pmatrix} E_{\vartheta in} \\ E_{\varphi in} \end{pmatrix}$$

It describes the relation between the input signal (E_{in} near the transmitter) and the output signal (E_{out} at the receiver). The transmission matrix is computed for each propagation path and can later be used to analyze the channel of the scenario in detail.

III. EXAMPLE

The example presented in this paper is a typical suburban Car-2-Car scenario. In Fig. 6 a small part of the environment is shown. The transmitting antenna (isotropic, 5.9 GHz) is located on the front of the red vehicle. The receiving antenna is mounted at the front of the blue car. All vehicles in this scenario are time variant, this means they are driving along the road course with different velocities and several acceleration/deceleration procedures. Each of the vehicles is defined by 20 RCS scattering centers (see Fig. 3). The polygons of the car models are not considered for the determination of reflection and diffraction points during the computation, as these two phenomena are already included in the RCS modeling. Polygons are only used for shadowing effects, e.g. the computation of the transmission loss, if a propagation path penetrates a car.

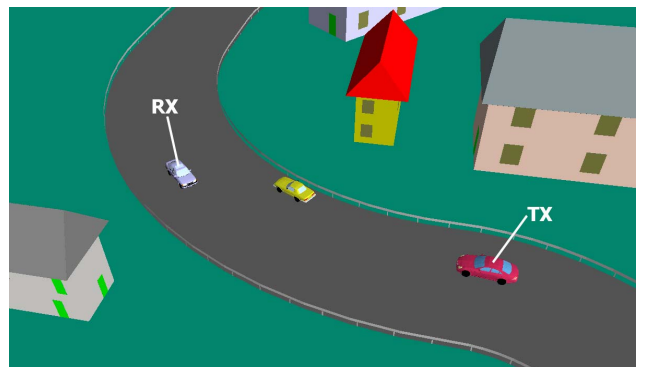


Fig. 6: A Car-to-Car Communication scenario. The transmitter is located on the front of the red car and the receiver on the front of the blue car.

Vector oriented road courses (streets with guard rails) are automatically generated based on tables with information about the road layout: Straight street parts as well as curves can be defined and inserted to a list which is then used to create the course automatically (based on parameters like street width, number of lanes,...).

Buildings, bridges, tunnels and other objects can also be included in time variant scenarios. These objects are available in 3D CAD files.

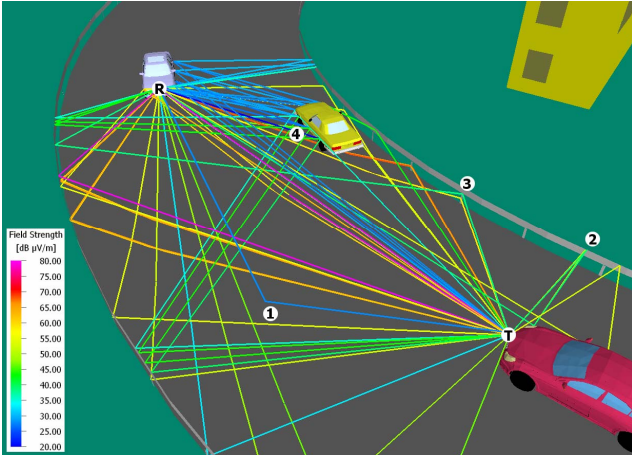


Fig. 7: Some of the computed propagation paths are shown in this figure. T indicates the transmitter, R the receiver. Some propagation phenomena are marked, such as scattering on the road surface (1), diffraction (2), reflection (3) and scattering on RCS (4).

A prediction result for $t=6.5s$ is shown in Fig. 7. Only the most relevant propagation paths are shown (about 50). The color of each propagation path indicates the strength of its contribution to the CIR (see legend). Examples for the different propagation phenomena considered by the algorithm are marked in the picture.

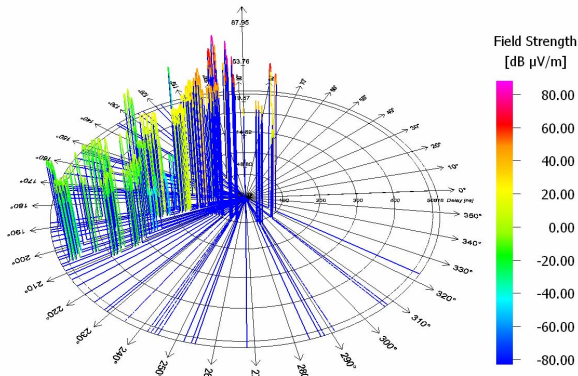


Fig. 8: Predicted spatial CIR for $t=6.5s$.

The computation time is less than 10 minutes per snapshot. The algorithm is an appropriate approach, so there is still much room for improving the computation time in future. In this example a maximum of two reflections, one diffraction, two scatterings at RCS or at the road surface are computed for each propagation path. More interactions do not improve the accuracy significantly, as further propagation paths with a higher number of interactions are highly attenuated and do not deliver a relevant contribution to the CIR. All elements in the database with their individual material properties (buildings, streets, guardrails)

are considered during the computation.

Fig. 8 shows the predicted spatial CIR for the same snapshot time ($t=6.5s$). In this figure all propagation paths are displayed, not only the most relevant ones as in Fig. 7. The two major contributions to the CIR are the direct ray (Line-Of-Sight) and the reflected ray on the guardrail. Scatterings on vehicles (modeled with RCS) deliver also relevant contributions to the CIR, as most of the car body is built of metal.

IV. COMPARISON TO MEASUREMENTS

A. Channel Impulse Response

A comparison of measured and predicted Channel Impulse Responses is used to validate the new approach. Wideband measurements have been made for several locations in a modern office building [15] in the 4 GHz band. These measurements are ideally suited to validate the new approach. Fig. 9 shows a map of the building. The transmitter location is marked in the map.

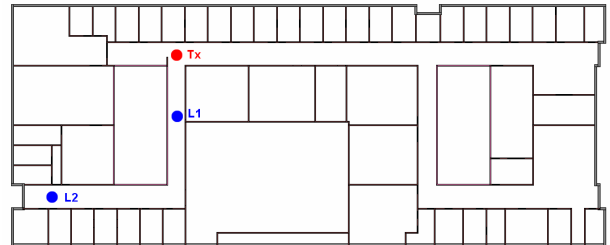


Fig. 9: The modern office building with transmitter (red) and measurement points for the CIR (blue).

In the following the prediction results for the CIR for two receiver locations (L1 and L2) are evaluated. The Fig. 10 shows comparisons of measured and predicted CIR for both L1 and L2. L1 is a LOS situation, that is the reason why the impulse at about $t=30$ ns is much higher than the other ones following. L2 is a NLOS situation – because of that the difference between strongest and weakest impulse is rather small. The different scales of both figures should be noticed.

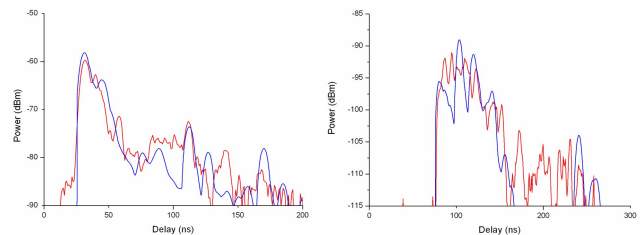


Fig. 10: Comparison of measured (red) and predicted (blue) channel impulse response for receiver location L1 (left) and L2.

The quite good accordance of measured and predicted CIR can be seen in Figure 10.

B. Delay Spread

In a second step, Delay Spread predictions are compared against data from spatially resolved wideband radio channel measurements. Measurements were done in different propagation scenarios in a modern office building (see Fig.

11). On contrary to older buildings made of brick and concrete, in this building outer walls were mainly made of glass, and inner walls were mostly soft partitions.

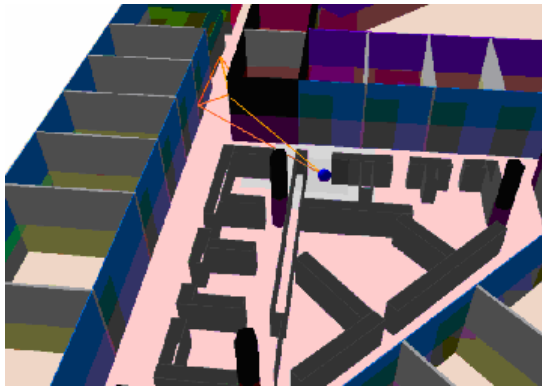


Fig. 11: A part of the modern office building, where the Delay Spread measurement campaign was accomplished.

The transmitter was located in an open plan office area or inside a meeting room. The amount of furniture varies from moderate to dense. The receiver is moving in the same floor inside offices and along corridors both in LOS and NLOS to the transmitter.

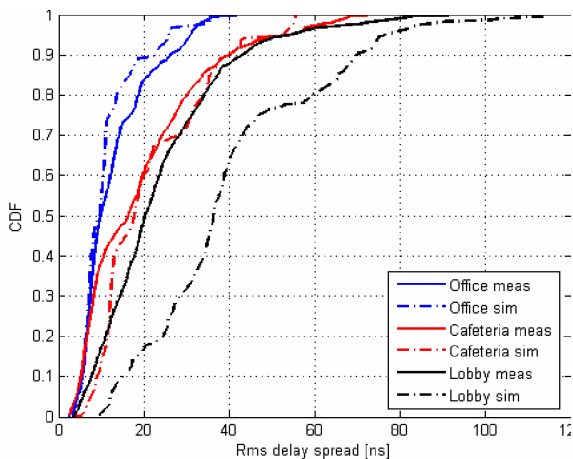


Fig. 12: Measured and simulated CDF for rms delay spread in different locations.

There are different approaches to compare measured and simulated channel characteristics. If rms delay spreads are calculated from matched filter outputs, the measurement system bandwidth affects the resulting values. In order to make meaningful comparisons, ray tracing impulse responses should be filtered to match the measurement bandwidth. In this approach the super-resolution outputs were directly compared against ray tracing simulations without filtering. This approach benefits from computational simplicity.

Fig. 12 shows the cumulative distribution functions for measured and predicted rms delay for three different parts of the scenario: Office, cafeteria and lobby. Smallest delay spread values were measured in office environment, ~ 5 -25 ns, and the simulated delay spread values are well in the same range. In cafeteria and lobby scenarios the measured delay spread values were somewhat greater, ~ 5 -40 ns. The ray tracing prediction could produce similar statistics in cafeteria scenario, but for lobby scenario there is a discrepancy between measurements and simulations.

V. CONCLUSIONS

In this paper the requirements for modeling the radio channel in large time variant wireless ad-hoc networks are described. A ray tracing approach for the propagation modeling in such scenarios is presented. Concepts for the substitution of vehicles with radar cross sections and for the modeling of scattering on rough surfaces are shown. The performance of the new Ray Tracing algorithm is successfully validated with a comparison from prediction to measurements of typical channel characteristics, such as Channel Impulse Response and Delay Spread.

Up to now costly measurement campaigns are needed to determine the spatial CIR in time variant scenarios. Simulations now offer the possibility to modify a time variant scenario and resimulate the CIR within short time intervals instead of carrying out time-consuming measurement campaigns.

VI. REFERENCES

- [1] D. DIDASCALOU, M. YOUNIS and W. WIESBECK: Millimeter wave propagation mechanisms for mobile intervehicle communications, Proc. EUNARV'98 Vehicle Navigation - ITS ready for market?, Hannover, Germany, pp. 81-90, June 1998
- [2] CAR 2 CAR COMMUNICATION CONSORTIUM: Mission and Objectives, www.car-2-car.org
- [3] M. VELDHORST: An analysis of sparse matrix storage schemes, Amsterdam : Mathem. Centrum, 1982
- [4] FGAN - Forschungsgesellschaft für Angewandte Naturwissenschaften e.V., www.fgan.de
- [5] G. T. RUCK: Radar cross section handbook, 1970
- [6] K. SCHULER, R. LENZ, D. BECKER, W. WIESBECK: Extraction of Scattering Centers of Vehicles by Ray-Tracing Simulations, 4th International Workshop on Intelligent Transportation, Hamburg, Germany, 2007.
- [7] F. WEINMANN, T. F. EIBERT: Radar Cross Section Modelling of Large Complex Objects, Kleinheubacher Tagung, 2005.
- [8] N. YAMADA: Radar Cross Section for Pedestrian in 76 GHz Band, R&D Review of Toyota CRDL, 2004.
- [9] G. L. JAMES: Geometrical theory of diffraction for electromagnetic waves. Stevenage : Peregrinus, 1986.
- [10] G. WOELFLE: Adaptive Propagation Models for the Planning of Wireless Communication Networks and for the Computation of the Reception Quality inside Buildings, PhD thesis, University of Stuttgart, Shaker-Verlag, 2000.
- [11] J. VANDAMME, S. BARANOWSKI, P. MARIAGE: High Frequency Diffraction by a Dielectric Wedge, PIMRC 1995, Toronto, Ont., Canada.
- [12] T. P. GILL: The Doppler effect. London: Logos Pr., 1965.
- [13] N. GENG, W. WIESBECK: Planungsmethoden für die Mobilkommunikation, Springer Verlag 1998
- [14] F. T. ULABY, M.C. DOBSON: Handbook of Radar Scattering Statistics for Terrain. Artech House, Norwood, 1989.
- [15] S. Y. SEIDEL, T. S. RAPPAPORT: Site-Specific Propagation Prediction for Wireless In-Building Personal Communication System Design, IEE Transactions on Vehicular Technology, Vol. 43, No. 4, 1994.